Journal of Solid State Chemistry 182 (2009) 1673–1678

Contents lists available at ScienceDirect

Journal of Solid State Chemistry

journal homepage: www.elsevier.com/locate/jssc

Reduction of Eu^{3+} to Eu^{2+} in $MAl_2Si_2O_8$ (M = Ca, Sr, Ba) in air condition

Cuimiao Zhang [a,b], Jun Yang [a,b], Cuikun Lin [a], Chunxia Li [a], Jun Lin [a,*]

[a] State Key Laboratory of Rare Earth Resource Utilization, Changchun Institute of Applied Chemistry, Chinese Academy of Sciences, 5625 Remin Street, Changchun 130022, PR China
[b] Graduate University of the Chinese Academy of Sciences, Beijing 100049, PR China

ARTICLE INFO

Article history:
Received 13 November 2008
Received in revised form
4 April 2009
Accepted 7 April 2009
Available online 15 April 2009

Keywords:
$MAl_2Si_2O_8$ (M = Ca
Sr
Ba)
Photoluminescence
Cathodoluminescence
Reduction

ABSTRACT

In general, the reduction of Eu^{3+} to Eu^{2+} in solids needs an annealing process in a reducing atmosphere. In this paper, it is of great interest and importance to find that the reduction of Eu^{3+} to Eu^{2+} can be realized in a series of alkaline-earth metal aluminum silicates $MAl_2Si_2O_8$ (M = Ca, Sr, Ba) just in air condition. The Eu^{2+}-doped $MAl_2Si_2O_8$ (M = Ca, Sr, Ba) powder samples were prepared in air atmosphere by Pechini-type sol–gel process. It was found that the strong band emissions of $4f^65d^1$–$4f^7$ from Eu^{2+} were observed at 417, 404 and 373 nm in air-annealed $CaAl_2Si_2O_8$, $SrAl_2Si_2O_8$ and $BaAl_2Si_2O_8$, respectively, under ultraviolet excitation although the Eu^{3+} precursors were employed. In addition, under low-voltage electron beam excitation, Eu^{2+}-doped $MAl_2Si_2O_8$ also shows strong blue or ultraviolet emission corresponding to $4f^65d^1$–$4f^7$ transition. The reduction mechanism from Eu^{3+} to Eu^{2+} in these compounds has been discussed in detail.

1. Introduction

It is well known that divalent europium ions (Eu^{2+}) have been widely used as activators in phosphor materials [1–6]. Much attention has been paid to the luminescent properties of Eu^{2+} ions in various matrix compounds and the reduction processes of Eu^{3+} to Eu^{2+} in phosphor preparations [7–12]. The Eu^{2+} ions show broad emission bands ranging from ultraviolet (UV) to red spectral region arising from interconfigurational $4f^65d^1$–$4f^7$ allowed transition. This is strongly dependent on the crystal fields of the host lattices since 5*d* orbitals are more sensitive to the ligand field. Accordingly, the Eu^{2+} becomes a very useful activator in phosphors for applications in displays, lamps and luminescent paintings [4]. In general, the reduction of Eu^{3+} to Eu^{2+} in solids needs an annealing process in a reducing atmosphere such as H_2, H_2/N_2 mixture or CO. If the reduction of Eu^{3+} to Eu^{2+} can be realized in air condition, it would greatly reduce the cost and increase the safety in preparing of Eu^{2+}-activated phosphor materials. So far, the reduction of Eu^{3+} to Eu^{2+} in air condition has been realized only in a very limited compounds, such as SrB_4O_7 [3], $Ba_3(PO_4)_2$ [9], $BaMgSiO_4$ [10], $Sr_4Al_{14}O_{25}$ [11], $ZnO–B_2O_3–P_2O_5$ glasses [12], and so on. As a result, it would be very important to find other host compounds in which Eu^{3+} can be reduced to Eu^{2+} in air condition (without reducing atmosphere).

Feldspars are naturally occurring aluminosilicates, constituting one of the most groups of minerals found in the Earth's crust. In alkaline-earth feldspars $MAl_2Si_2O_8$ (where M = Ca, Sr, Ba), the framework structures are formed from an array of interlinked corner-sharing SiO_4 and AlO_4 tetrahedra, with Al charge-compensating cations Ca, Sr, Ba occupying the large cavities within the structure. These systems are underpinned by significant theoretical understanding, due to their commercial significance in the electronics and chemical industries [13–15]. A solid solution series of isostructural members with slightly different sized cations as hosts [such as $MAl_2Si_2O_8$ (M = Ca, Sr, Ba)] would be an ideal system to study the effect of crystal chemical variation on the luminescence of Eu^{2+} ions [14]. Moreover, it offers the possibilities in finding the useful Eu^{2+}-$MAl_2Si_2O_8$ phosphors for commercial applications.

Pechini-type sol–gel process (PSG, also known and called as polymerizable-complex technique), is well known and extensively used for the design and synthesis of advanced functional and engineering materials, including films, fibers, monoliths, and powders of almost any shape, size, and chemical composition. The PSG process reduces segregation of particular metal ions and ensures compositional homogeneity [16]. This method can overcome most of the difficulties and disadvantages that frequently occur in solid-state method and the alkoxides based sol–gel process. For instance, long calcination time, or multiple sintering at high temperature may frequently occur in the solid-state process; most of metal alkoxides suffer from high cost, unavailability, toxicity, and fast hydrolysis rate during sol–gel process [17]. In the past five years, we have extended the application of the PSG process to the systematic synthesis of various kinds of optical materials, including luminescent powders, thin films, core-shell structured phosphors, and pigments [18–23].

* Corresponding author. Fax: +86 431 85698041.
E-mail address: jlin@ciac.jl.cn (J. Lin).

0022-4596/$ - see front matter © 2009 Elsevier Inc. All rights reserved.
doi:10.1016/j.jssc.2009.04.009

In this paper, a series of alkaline-earth metal aluminum silicates $MAl_2Si_2O_8$ (M = Ca, Sr, Ba) samples were prepared by PSG process. We have found that the reduction of Eu^{3+} to Eu^{2+} can well be realized in $MAl_2Si_2O_8$ (M = Ca, Sr, Ba) in air condition. The resulted $MAl_2Si_2O_8$:Eu phosphors show strong band emission from 350 to 550 nm of Eu depending on the kind of alkaline-earth metal in the compounds. The reduction mechanism and the luminescent properties of $MAl_2Si_2O_8$:Eu samples have been discussed in detail.

2. Experimental section

Materials. The rare earth oxide Eu_2O_3 (99.999%) was purchased from Yuelong New Materials Co., Ltd., and other chemicals were purchased from Beijing Chemical Corporation. All chemicals are of analytical grade reagents and used directly without further purification.

Preparation. The $MAl_2Si_2O_8$:Eu (M = Ca, Sr, Ba) powder samples were prepared by a PSG process [16]. Firstly, the Eu_2O_3 was dissolved in dilute HNO_3 under stirring and heating, resulting in the formation of a colorless solution of $Eu(NO_3)_3$. The doping concentration of Eu was chosen as 2–14% (molar ratio) in $MAl_2Si_2O_8$:Eu. In a typical procedure, stoichiometric amounts of $Ca(NO_3)_2 \cdot 4H_2O$ [$Sr(NO_3)_2$ or $Ba(NO_3)_2 \cdot 2H_2O$], $Al(NO_3)_3 \cdot 9H_2O$, $Eu(NO_3)_3$ and tetraethoxysilane $Si(OC_2H_5)_4$ were dissolved in a water/ethanol (v/v = 2:1) solution under vigorous stirring. Then certain amount of citric acid (citric acid/M^{2+} = 2:1, molar ratio) and polyethylene glycol (PEG, 10 000; 0.1 g/mL) were added into the above solution. The resultant mixture was stirred for 3 h and heated at 90 °C in a water bath until homogeneous gels formed. After being dried, the obtained gels were prefired at 500 °C for 3 h, fully ground, and then annealed at 1400 °C for 3 h in air atmosphere to produce the final samples.

Characterization. The X-ray diffraction (XRD) of powder samples was examined on a Rigaku-Dmax 2500 diffractometer using Cu$K\alpha$1 radiation (λ = 0.15405 nm). The photoluminescence (PL) excitation and emission spectra were taken on an F-4500 spectrophotometer equipped with a 150 W xenon lamp as the excitation source. Luminescence lifetimes were measured with a Lecroy Wave Runner 6100 digital oscilloscope (1 GHz) using 310 nm lasers (pulse width = 4 ns) as the excitation source (Continuum Sunlite OPO). Electron paramagnetic resonance (EPR) spectra were taken on the JES-FE3AX electronic spin resonance spectrophotometer. The cathodoluminescent (CL) measurements were carried out in an ultra-high-vacuum chamber (<10–8 torr), where the samples were excited by an electron beam at a voltage range of 1–3 kV with different filament currents, and the spectra were recorded on an F-4500 spectrophotometer. All the measurements were performed at room temperature.

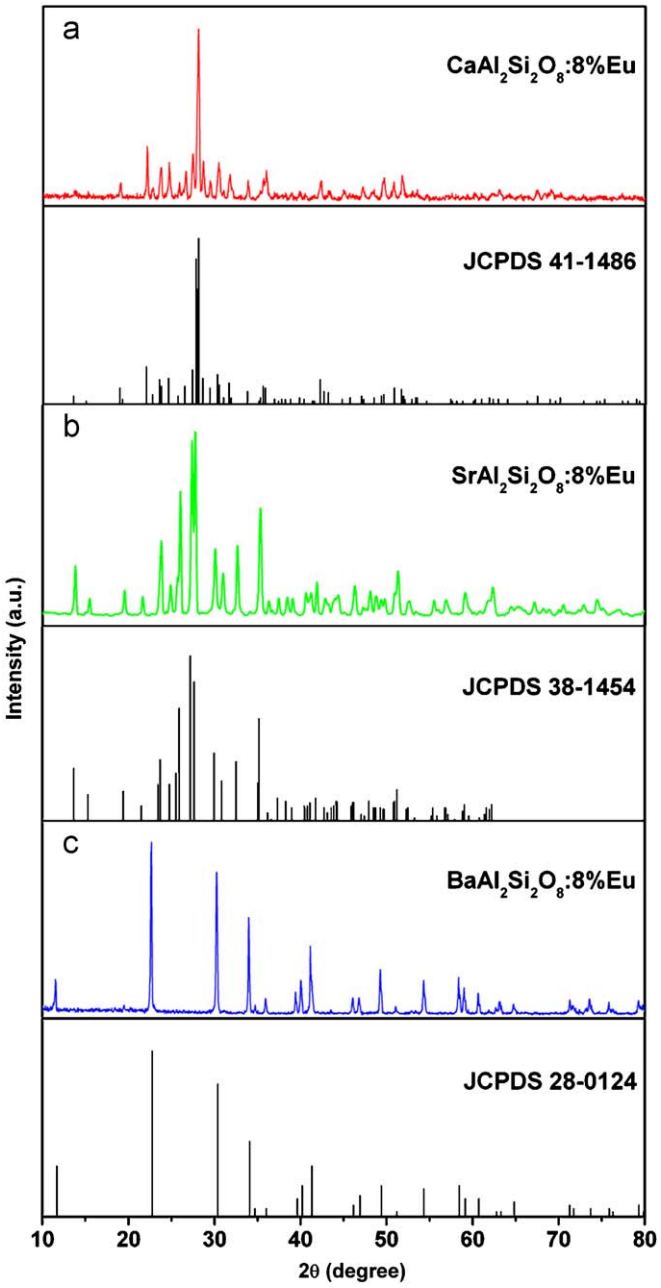

Fig. 1. XRD patterns of $CaAl_2Si_2O_8$:Eu^{2+} (a), $SrAl_2Si_2O_8$:Eu^{2+} (b), $BaAl_2Si_2O_8$:Eu^{2+} (c), and the standard datas of $CaAl_2Si_2O_8$ (JCPDS 41–1486), $SrAl_2Si_2O_8$ (JCPDS 38–1454), and $BaAl_2Si_2O_8$ (JCPDS 28–0124) as a reference. All samples were obtained after annealing at 1400 °C in air and with the initial europium concentration equal to 8 mol%.

3. Results and discussion

XRD. Fig. 1 shows the XRD patterns for the $MAl_2Si_2O_8$:Eu (M = Ca, Sr, Ba) samples annealing at 1400 °C in air: (a) $CaAl_2Si_2O_8$:Eu^{2+}, (b) $SrAl_2Si_2O_8$:Eu^{2+}, and (c) $BaAl_2Si_2O_8$:Eu^{2+}, respectively. All samples were obtained after annealing at 1400 °C in air and with the initial europium concentration of 8 mol%. It is clear from Fig. 1 that all the diffraction peaks of three europium-doped compounds can be readily indexed to the corresponding standard data for triclinic phase of $CaAl_2Si_2O_8$ (JCPDS 41–1486; space group: $P1$ No. 2), monoclinic phase of $SrAl_2Si_2O_8$ (JCPDS 38–1454; space group: $C2/m$ No. 12) and hexagonal phase of $BaAl_2Si_2O_8$ (JCPDS 28–0124; space group: $P3$, No. 147), respectively. No other impurities can be detected. Essentially, the structures of alkaline-earth metal aluminum silicates are based on an infinite three-dimensional silicon–oxygen and aluminum–oxygen frameworks, which are formed from interlinked corner-sharing AlO_4 and SiO_4 tetrahedra [6,13–15]. The differences in crystal symmetries of the three samples may be attributed to the difference in size of the alkaline-earth metal ions around which the framework closes in [14]. In $MAl_2Si_2O_8$ (M = Ca, Sr, Ba), half of the tetrahedral positions in the framework are occupied by Al^{3+} and the other half by Si^{4+}. So that, for every two Al^{3+}, one divalent Ca^{2+}, Sr^{2+}, or Ba^{2+} is introduced to neutralize the negative charge of the framework.

Photoluminescence properties. Although the precursor for europium was trivalent from $Eu(NO_3)_3$ and the samples were prepared

by annealing at 1400 °C in air condition, it seems that the europium exists in divalent state in all the three compounds. This can be confirmed directly by the photoluminescence excitation and emission spectra of the samples. Parts a and b of Fig. 2 show the excitation and emission spectra of $CaAl_2Si_2O_8$:Eu^{2+} (red line), $SrAl_2Si_2O_8$:Eu^{2+} (blue line) and $BaAl_2Si_2O_8$:Eu^{2+} (black line) samples with the initial europium concentration of 8 mol%, respectively. For $CaAl_2Si_2O_8$:8% Eu sample, the emission spectrum consists of a strong broad band ranging from 375 to 550 nm with a maximum at 417 nm, and the corresponding excitation spectrum includes a broad band from 200 to 400 nm with a maximum at 324 nm with several shoulders at 275, 324, 350 nm (the shoulder peaks are not obvious because the scale of ordinate in Fig. 2a is too large). It can be concluded from the spectra that these band spectral properties are the characteristic of Eu^{2+} [8], but not the Eu^{3+}. The excitation and emission spectra of Eu^{3+} generally consist of sharp lines from 200 to 500 nm and from 550 to 750 nm, respectively, corresponding to the *f*–*f* transitions [24]. However, in fact, a very weak emission of Eu^{3+} could be observed from the enlarged emission spectra (not shown here). Therefore, it can be seen clearly that most of the Eu^{3+} has been reduced to Eu^{2+} during the annealing process, while a very small amount of Eu^{3+} also exists. The intense broad band centered at 417 nm can be attributed to the typical $4f^65d^1$ (t_{2g})–$4f^7$ ($^8S_{7/2}$) transition of Eu^{2+}, and the excitation bands can be attributed to the transitions from ground state of Eu^{2+} ($^8S_{7/2}$) to the different crystal field splitting components of $4f^65d^1$ state. The same situation holds for $SrAl_2Si_2O_8$:8% Eu and $BaAl_2Si_2O_8$:8% Eu samples, as shown in Fig. 2. The emission bands of $SrAl_2Si_2O_8$:8% Eu and $BaAl_2Si_2O_8$:8% Eu are located at 404 and 373 nm, and the corresponding peak position of the excitation bands are 328 (strong), 273 nm (weak) for the former and 244, 307 and 330 nm for the latter, respectively. These excitation and emission spectra can effectively confirm the reduction from Eu^{3+} to Eu^{2+} during the annealing process in air. As a reference, the excitation and emission spectra of commercial blue-emitting phosphor $BaMgAl_{10}O_{17}$:Eu^{2+}/Mn^{2+} (BAM:Eu^{2+}/Mn^{2+}) is also shown in Fig. 2 (green line). Compared with BAM: Eu^{2+}/Mn^{2+}, the present synthesized $CaAl_2Si_2O_8$:Eu^{2+} phosphor shows relatively weaker emission intensity, the $SrAl_2Si_2O_8$:Eu^{2+} phosphor almost has the same emission intensity, and the $BaAl_2Si_2O_8$:Eu^{2+} exhibits much stronger emission intensity (Fig. 2b). In addition, as can be seen in Fig. 2b, the main emission peaks of the Eu^{2+}-activated $CaAl_2Si_2O_8$, $SrAl_2Si_2O_8$, and $BaAl_2Si_2O_8$ shift gradually to shorter wavelength from 417 to 373 nm. This blue shift behavior can be explained by the change of the crystal field [1,6,14,25–27]. Because ionic radius (Ca^{2+}, Sr^{2+}, Ba^{2+}) and structure are very different, the crystal field intensity around Eu^{2+} in $CaAl_2Si_2O_8$, $SrAl_2Si_2O_8$, and $BaAl_2Si_2O_8$ decreases along with the order of Ca, Sr, and Ba [1,2,26,27]. Therefore, the lowest 5*d* levels of Eu^{2+} in $CaAl_2Si_2O_8$:Eu^{2+} and $SrAl_2Si_2O_8$:Eu^{2+} would become lower than that of $BaAl_2Si_2O_8$:Eu^{2+}. The crystal field splitting of 5*d* levels for $Eu^{2+}$and the emission process are shown in Fig. 3.

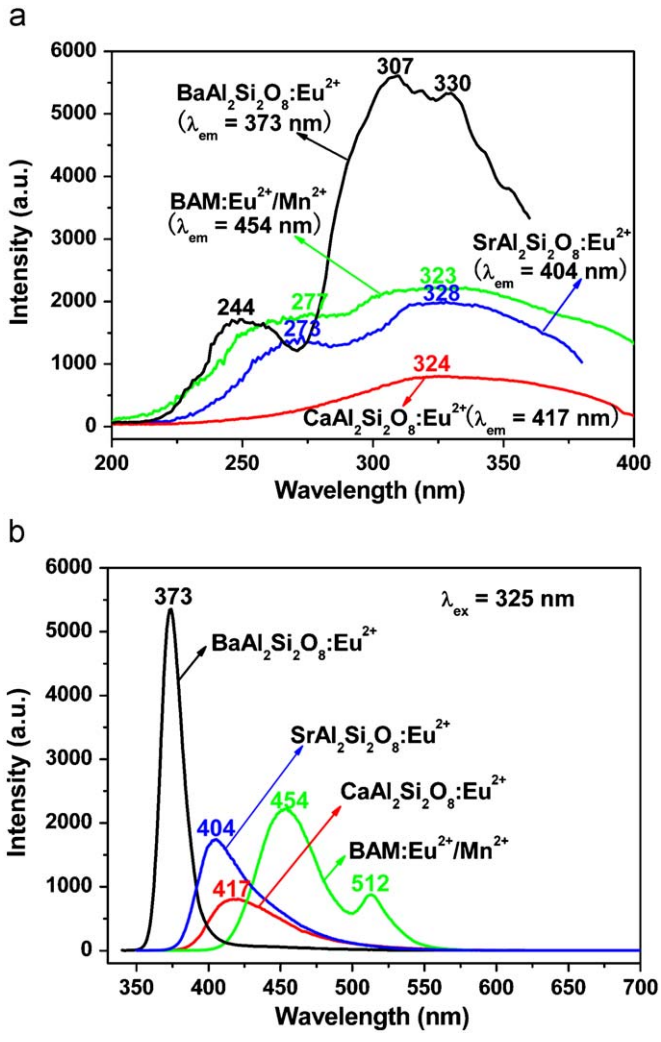

Fig. 2. Excitation (a) and emission (b) spectra for $CaAl_2Si_2O_8$:Eu^{2+} (red line), $SrAl_2Si_2O_8$:Eu^{2+} (blue line), $BaAl_2Si_2O_8$:Eu^{2+} (black line) and commercial blue-emitting phosphor BAM: Eu^{2+}/Mn^{2+} (green line). (for interpretation of the references to color in this figure legend, the reader is referred to the web version of this article.)

The luminescence decay curves for $CaAl_2Si_2O_8$:Eu^{2+} (a), $SrAl_2Si_2O_8$:Eu^{2+} (b), and $BaAl_2Si_2O_8$:Eu^{2+} (c) are shown in Fig. 4. All of the three samples can be fitted to a single-exponential function as $I(t) = A\exp(-t/\tau)$ (where τ is the lifetime) [28]. The lifetimes for the emission of $CaAl_2Si_2O_8$:Eu^{2+} (417 nm), $SrAl_2Si_2O_8$:Eu^{2+} (404 nm) and $BaAl_2Si_2O_8$:Eu^{2+} (373 nm) are 0.416 μs (Fig. 4a), 0.496 μs (Fig. 4b) and 0.848 μs (Fig. 4c), respectively. The luminescence decay behaviors and the lifetimes for the samples are the characteristic of Eu^{2+} ions [1,28], which are in accordance with the photoluminescence results. The reduction of Eu^{3+} to Eu^{2+} in $MAl_2Si_2O_8$ (M = Ca, Sr, and Ba) during the annealing process in air condition can be further confirmed.

The difference between the electronic configuration of the Eu^{2+} ions and that of Eu^{3+} ions exists: the Eu^{2+} ions have paramagnetic property ($4f^7$, $S = 7/2$, $L = 0$, $J = 7/2$), while the Eu^{3+} ions do not have it ($4f^6$, $S = 3$, $L = 3$, $J = 0$) [6,29,30]. In order to get definite proof for the presence of Eu^{2+} ions, EPR analysis was performed on Eu-doped $CaAl_2Si_2O_8$, $SrAl_2Si_2O_8$, and $BaAl_2Si_2O_8$, respectively. Fig. 5 shows the EPR spectra of $CaAl_2Si_2O_8$:Eu^{2+} (red line),

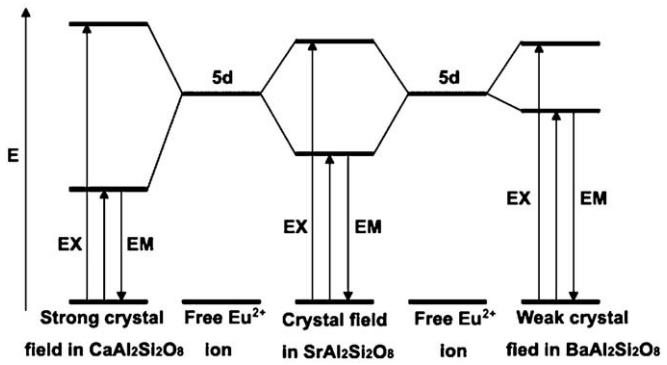

Fig. 3. Schematic diagram for Eu^{2+} energy levels in $CaAl_2Si_2O_8$, $SrAl_2Si_2O_8$, and $BaAl_2Si_2O_8$ crystal fields.

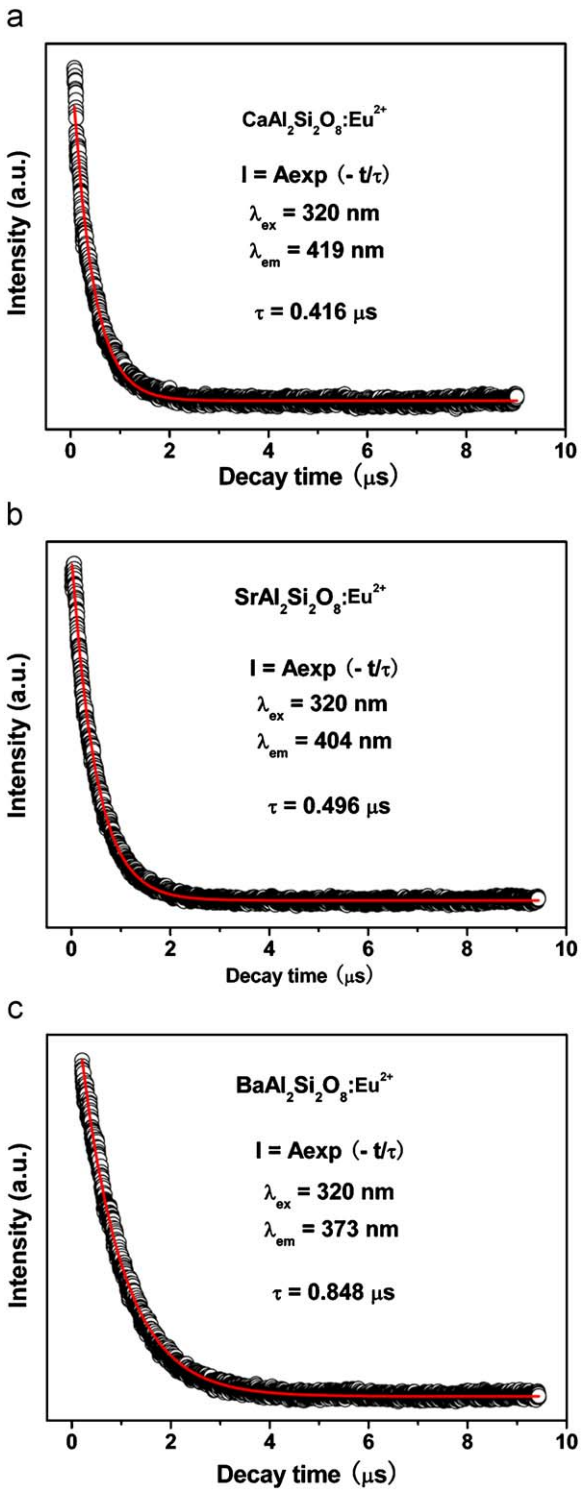

Fig. 4. The decay curves for the luminescence of sol–gel-derived $CaAl_2Si_2O_8:Eu^{2+}$ (a), $SrAl_2Si_2O_8:Eu^{2+}$ (b), $BaAl_2Si_2O_8:Eu^{2+}$ (c) samples with the initial europium concentration equal to 8 mol%.

$SrAl_2Si_2O_8:Eu^{2+}$ (blue line), and $BaAl_2Si_2O_8:Eu^{2+}$ (black line) samples. In EPR spectra, pronounced features (effective *g*-values of 3.3 for $CaAl_2Si_2O_8:Eu^{2+}$, 2.6 for $SrAl_2Si_2O_8:Eu^{2+}$, and 1.7 for $BaAl_2Si_2O_8:Eu^{2+}$, respectively) are observed. So we can confirm that the reduction of Eu^{3+} to Eu^{2+} indeed took place in the as-prepared $MAl_2Si_2O_8$:Eu samples during the preparation in air at high temperature.

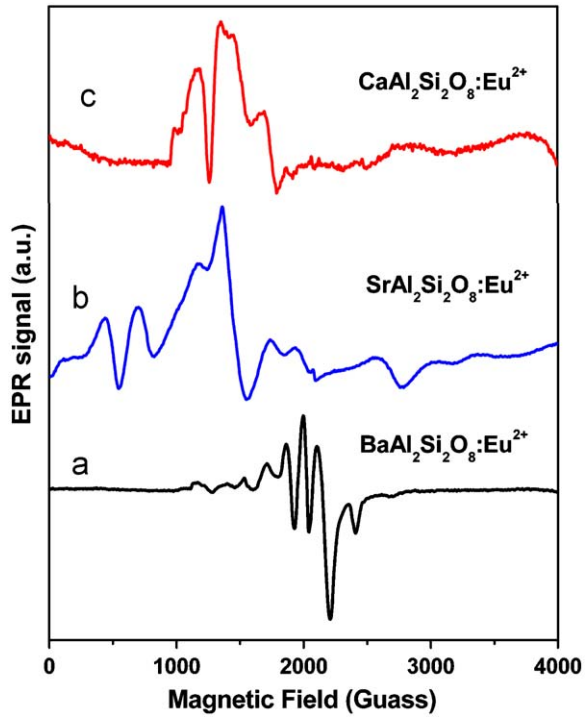

Fig. 5. The EPR spectra for PEG-derived $CaAl_2Si_2O_8:Eu^{2+}$ (a), $SrAl_2Si_2O_8:Eu^{2+}$ (b), and $BaAl_2Si_2O_8:Eu^{2+}$ (c).

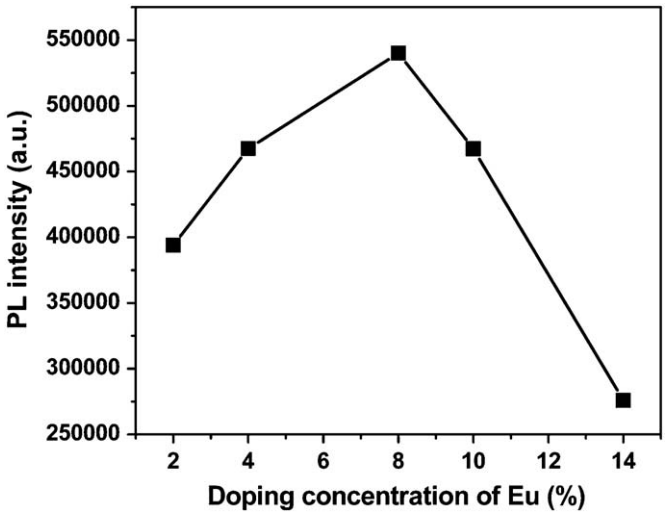

Fig. 6. The emission intensity of sol–gel-derived $SrAl_2Si_2O_8:Eu^{2+}$ as a function of initial europium doping concentration (molar ratio).

To understand and optimize the luminescent properties of $MAl_2Si_2O_8$:Eu luminescent materials, the experiments of different doping concentration of Eu were performed on $SrAl_2Si_2O_8:Eu^{2+}$ as representative of $MAl_2Si_2O_8$:Eu. It is found that the PL intensities for the emission spectra clearly vary with the change of Eu-doping concentration, as shown in Fig. 6. The critical doping concentration of Eu was experimentally studied to optimize the photoluminescence of the $SrAl_2Si_2O_8:Eu^{2+}$ phosphors. It indicates that the PL intensity of the phosphor is strongly influenced by the activator concentration [20,31,32]. The PL intensity first increases with increasing activator concentration, reaching a maximum value at 8%, then decreases quickly with further increasing the doping concentration (Fig. 6). This result can be attributed to the

concentration quenching of activator ions. Thus, the optimum Eu-doping concentration is about 8% for obtaining the strongest PL emission intensity. Moreover, we take the $SrAl_2Si_2O_8$:8% Eu sample as a example to investigate the influence of annealing temperature. It can be found that the all the diffraction peaks agree well with the monoclinic phase of $SrAl_2Si_2O_8$ when the samples were annealed at 1400 °C or higher. When the annealing temperature was at 1300 °C, however, some minor impurity peaks appear in the range of 30–35°, which can be attributed to the unreacted component at low temperature. Moreover, the exitation and emission spectra of the samples are very similar when annealed at different temperature. So we choose the annealing temperature is 1400 °C for other samples.

Cathodoluminescence properties. Under low-voltage electron beam excitation, the sol–gel-derived $CaAl_2Si_2O_8:Eu^{2+}$, $SrAl_2Si_2O_8:Eu^{2+}$, and $BaAl_2Si_2O_8:Eu^{2+}$ samples exhibit strong blue and ultraviolet emission, respectively. The typical cathodoluminescence (CL) emission spectra of $MAl_2Si_2O_8$:8% Eu phosphors under the excitation of electron beams (accelerating voltage = 2.5 kV; filament current = 98 mA) are shown in Fig. 7. The CL emission spectra are similar to the corresponding PL emission spectra (Fig. 2b) except for a little red shift of each peak. The red shift may be caused by the different excitation mechanisms [33,34]. As representative of $MAl_2Si_2O_8$:Eu (M = Ca, Sr, Ba), the CL emission intensities for $CaAl_2Si_2O_8$:8% Eu phosphor has been investigated as a function of the accelerating voltage and the filament current, as shown in Fig. 8a and b, respectively. When the filament current is fixed at 98 mA, the CL intensity increases with raising the accelerating voltage from 1 to 3 kV (Fig. 8a). Similarly, under a 3 kV electron beam excitation, the CL intensity also increases with increasing the filament current from 89 to 101 mA (Fig. 8b). For cathodoluminescence, the Eu^{2+} ions are excited by the plasma produced by the incident electrons. The electron penetration depth can be estimated by

$$L[\text{Å}] = 250(A/\rho)(E/Z^{1/2})^n \quad (1)$$

where $n = 1.2/(1-0.29\log_{10}Z)$, A is the atomic or molecular weight of the material, ρ is the bulk density, Z is the atomic number or the number of electrons per molecule in the case compounds, and E is the accelerating voltage (kV) [35]. With the increase of accelerating voltage, more plasma will be produced by the incident electrons, resulting in more Eu^{2+} being excited and higher CL intensity. The increase in electron energy is attributed to deeper penetration of electron into the phosphor body which is governed by Eq. (1). The deeper penetration of electrons in the phosphor body results in an increase in electron–solid interaction volume in which excitation of Eu^{2+} ions is responsible for the light emission [36]. The similar situation holds for $SrAl_2Si_2O_8$:8% Eu and $BaAl_2Si_2O_8$:8% Eu, respectively. Due to the strong low-voltage CL intensity of $MAl_2Si_2O_8$:Eu ($M = Ca^{2+}$, Sr^{2+}, and Ba^{2+}) phosphors, they are thought to fit into field emission display devices.

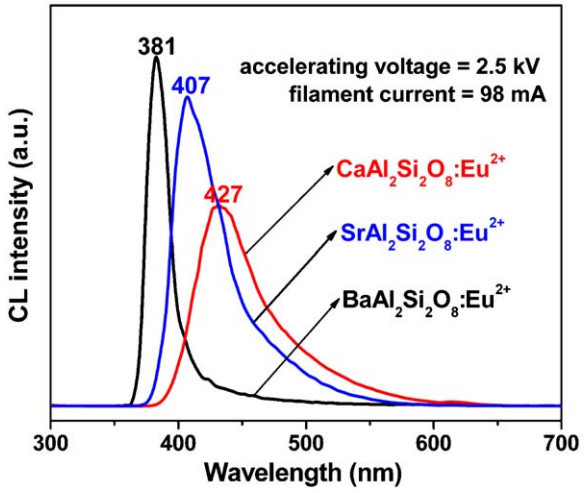

Fig. 7. Typical cathodoluminescence spectra of $CaAl_2Si_2O_8:Eu^{2+}$ (red line), $SrAl_2Si_2O_8:Eu^{2+}$ (blue line), and $BaAl_2Si_2O_8:Eu^{2+}$ (black line). (for interpretation of the references to color in this figure legend, the reader is referred to the web version of this article.)

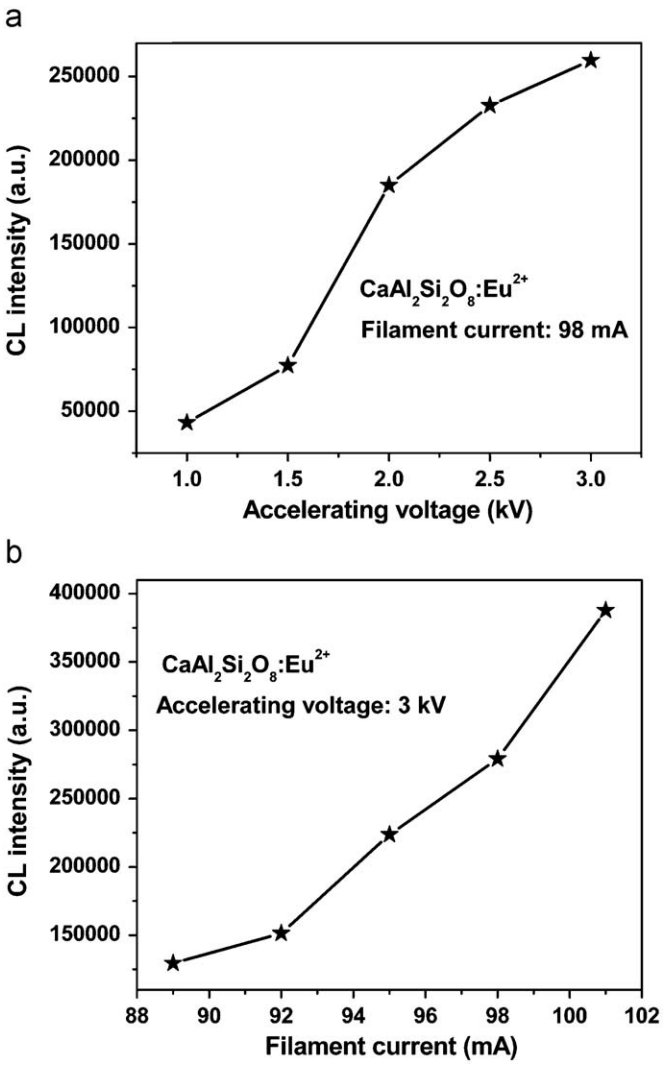

Fig. 8. The cathodoluminescence intensities of $CaAl_2Si_2O_8:Eu^{2+}$ as a function of accelerating voltage (a) and filament current (b).

The reduction of Eu^{3+} to Eu^{2+} in $MAl_2Si_2O_8$:Eu in air condition can be explained with the model of the charge compensation mechanism [3,10–12]. As trivalent Eu^{3+} ions are doped into $MAl_2Si_2O_8$, they replace M^{2+} ions. In order to maintain charge balance, two Eu^{3+} ions are needed to substitute for three M^{2+} ions. Hence, one vacancy defect V''_{Ca} (V''_{Sr} or V''_{Ba}) with two negative charges and two positive defects of $Eu_{Ca}^{\bullet}$ ($Eu_{Sr}^{\bullet}$ or $Eu_{Ba}^{\bullet}$) will be

Possible reduction mechanisms. When Eu^{2+} ions are incorporated into the crystal structures of $CaAl_2Si_2O_8$, $SrAl_2Si_2O_8$, or $BaAl_2Si_2O_8$, Eu^{2+} ions may substitute at all cationic site Ca^{2+} (Sr^{2+} or Ba^{2+}), Al^{3+}, and Si^{4+}. However, considering their respective ionic radii and allowed oxygen-coordination number, it is difficult for Eu^{2+} ions to substitute for Al^{3+} or Si^{4+} ions [37]. Therefore, it is clear and reasonable that Eu^{2+} ions substitute for only Ca^{2+} ions in $CaAl_2Si_2O_8$, Sr^{2+} ions in $SrAl_2Si_2O_8$, or Ba^{2+} ions in $BaAl_2Si_2O_8$.

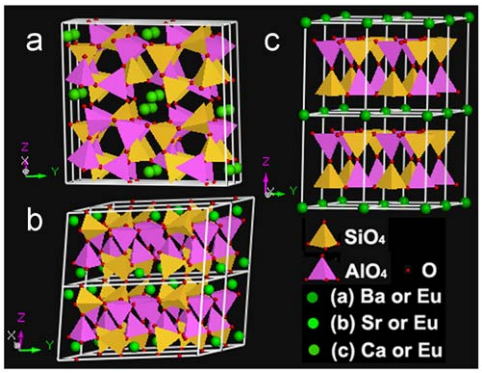

Fig. 9. The structures of aluminosilicate phosphors: (a) $CaAl_2Si_2O_8$:Eu, (b) $SrAl_2Si_2O_8$:Eu, and (c) $BaAl_2Si_2O_8$:Eu.

created by each substitution of every two Eu^{3+} ions in the compounds. The vacancy of V''_{Ca} (V''_{Sr} or V''_{Ba}) then acts as the donor of electrons, while the two $Eu^{\bullet}_{Ca}$ ($Eu^{\bullet}_{Sr}$ or $Eu^{\bullet}_{Ba}$) defects become acceptor of electrons. Consequently, by thermal stimulation, the negative charges in vacancy defects of V''_{Ca} (V''_{Sr} or V''_{Ba}) will be transferred to Eu^{3+} sites and reduce Eu^{3+} to Eu^{2+}. The whole process could be presented in the following equations:

$$3Ca^{2+}(Sr^{2+} \text{ or } Ba^{2+}) + 2Eu^{3+} = V''_{Ca}(V''_{Sr} \text{ or } V''_{Ba}) + 2Eu^{\bullet}_{Ca}(Eu^{\bullet}_{Sr} \text{ or } Eu^{\bullet}_{Ba}) \quad (2)$$

$$V''_{Ca}(V''_{Sr} \text{ or } V''_{Ba}) = V_{Ca}(V_{Sr} \text{ or } V_{Ba}) + 2e \quad (3)$$

$$2Eu^{\bullet}_{Ca}(Eu^{\bullet}_{Sr} \text{ or } Eu^{\bullet}_{Ba}) + 2e = 2Eu_{Ca}(Eu_{Sr} \text{ or } Eu_{Ba}) \quad (4)$$

In addition, the crystal structures of aluminosilicate phosphors also play a role of shield for Eu^{2+} against from oxidation during the annealing process. Fig. 9 shows the crystal structures of triclinic $CaAl_2Si_2O_8$:Eu (a), monoclinic $SrAl_2Si_2O_8$:Eu (b), and hexagonal $BaAl_2Si_2O_8$:Eu (c). Structurally, the framework of alkaline-earth metal aluminum silicates are formed from interlinked O-sharing AlO_4 and SiO_4 tetrahedra, with Al charge-compensating cations Ca^{2+}, Sr^{2+}, or Ba^{2+} occupying the large cavities available within the structure [6,13–15]. Since these reduced Eu^{2+} ions are located in the cavities of the three-dimensional network structure, they will be efficiently shielded from the influence of oxygen in ambient atmosphere. So the three compounds $CaAl_2Si_2O_8$, $SrAl_2Si_2O_8$, and $BaAl_2Si_2O_8$ can stabilize divalent europium ions.

4. Conclusions

In summary, the reduction process of Eu^{3+} to Eu^{2+} has been successfully observed in $CaAl_2Si_2O_8$, $SrAl_2Si_2O_8$, and $BaAl_2Si_2O_8$ samples prepared in air. It would greatly reduce the cost and increase the safety in preparing of Eu^{2+}-activated phosphor materials. The reduction process of Eu^{3+} to Eu^{2+} can be explained with the charge compensation model. The structures of three-dimensional networks composed by AlO_4 and SiO_4 tetrahedra are possible for occurrence of the reduction ($Eu^{3+} \rightarrow Eu^{2+}$) when samples were prepared in air at high temperature. Under the UV excitation, Eu^{2+}-activated $CaAl_2Si_2O_8$ and $SrAl_2Si_2O_8$ samples show strong blue emission centered at 417 and 404 nm, respectively, and the emission of Eu^{2+}-activated $BaAl_2Si_2O_8$ occurs in the ultraviolet region with a strong and narrow band centered at 373 nm. Similarly, under low-voltage electron beam excitation, the as-obtained $MAl_2Si_2O_8$:Eu ($M = Ca^{2+}$, Sr^{2+}, Ba^{2+}) samples exhibit strong blue and ultraviolet emission, respectively. Due to the excellent photoluminescence and cathodoluminescence performances, the $CaAl_2Si_2O_8$:Eu^{2+}, $SrAl_2Si_2O_8$:Eu^{2+}, and $BaAl_2Si_2O_8$:Eu^{2+} phosphors have potential for applications in light emitting diodes (LEDs), laser, and field emission displays (FEDs) devices.

Acknowledgments

This project is financially supported by National Basic Research Program of China (2007CB935502) and the National Natural Science Foundation of China (NSFC 50702057, 50872131, 00610227).

References

[1] G. Blasse, W.L. Wanmaker, J.W. Vrugt, A. Bril, Philips Res. Rep. 23 (1968) 189–200.
[2] S.H.M. Poort, W. Janssen, G. Blasse, J. Alloys Compd. 260 (1997) 93–97.
[3] Z.W. Pei, Q. Su, J.Y. Zhang, J. Alloys Compd. 198 (1993) 51–53.
[4] R. Stefani, A.D. Maia, E.E.S. Teotonio, M.A.F. Monteiro, M.C.F.C. Felinto, H.F. Brito, J. Solid State Chem. 179 (2006) 1086–1092.
[5] X. Piao, T. Horikawa, H. Hanzawa, K. Machida, Appl. Phys. Lett. 88 (2006) 161908–161913.
[6] W.B. Im, Y.K. Kim, D.Y. Jeon, Chem. Mater. 18 (2006) 1190–1195.
[7] S.H.M. Poort, W.P. Blokpoel, G. Blasse, Chem. Mater. 7 (1995) 1547–1551.
[8] S.H.M. Poort, J.W.H. van Krevel, R. Stomphorst, A.P. Vink, G. Blasse, J. Solid State Chem. 122 (1996) 432–435.
[9] I. Täle, P. Külis, V. Kronghauz, J. Lumin. 20 (1979) 343–347.
[10] M.Y. Peng, Z.W. Pei, G.Y. Hong, Q. Su, J. Mater. Chem. 13 (2003) 1202–1205.
[11] M.Y. Peng, Z.W. Pei, G.Y. Hong, Q. Su, Chem. Phys. Lett. 371 (2003) 1–6.
[12] Z.H. Lian, J. Wang, Y.H. Lv, S.B. Wang, Q. Su, J. Alloys Compd. 430 (2007) 257–261.
[13] A.E.R. Malins, N.R.J. Poolton, F.M. Quinn, O. Johnsen, P.M. Denby, J. Phys. D Appl. Phys. 37 (2004) 1439–1450.
[14] K.R. Laud, E.F. Gibbons, T.Y. Tien, H.L. Stadler, J. Electrochem. Soc. 118 (1971) 918–923.
[15] H.D. Grundy, Am. Mineral 59 (1974) 1319–1326.
[16] J. Lin, M. Yu, C.K. Lin, X.M. Liu, J. Phys. Chem. C 111 (2007) 5835–5845.
[17] N.Y. Turova, E.P. Turevakata, V.G. Kessler, M.I. Yanovskaya, The Chemistry of Metal Alkoxides, Kluwer Academic Publishers, Boston, MA, 2002.
[18] M. Yu, J. Lin, J. Fang, Chem. Mater. 17 (2005) 1783–1791.
[19] C.K. Lin, Y. Luo, H. You, Z.W. Quan, J. Zhang, J. Fang, J. Lin, Chem. Mater 18 (2006) 458–464.
[20] M. Yu, J. Lin, Z. Wang, J. Fu, S. Wang, H.J. Zhang, Y.C. Han, Chem. Mater. 14 (2002) 2224–2231.
[21] C.K. Lin, Y.Y. Li, M. Yu, P.P. Yang, J. Lin, Adv. Funct. Mater. 17 (2007) 1459–1465.
[22] H. Wang, C.K. Lin, X.M. Liu, J. Lin, M. Yu, Appl. Phys. Lett. 87 (2005) 181907–181909.
[23] M. Yu, J. Lin, J. Fu, H.J. Zhang, Y.C. Han, J. Mater. Chem. 13 (2003) 1413–1419.
[24] L.G. Deshazer, G.H. Dieke, J. Chem. Phys. 38 (1963) 2190–2199.
[25] T.J. Isaacs, J. Electrochem. Soc. 118 (1971) 1009–1011.
[26] Z.Y. Wang, Y.H. Wang, P.Y. Zhang, X.P. Fan, G.D. Qian, J. Lumin. 124 (2007) 140–142.
[27] J.S. Shi, Z.J. Wu, S.H. Zhou, S.Y. Zhang, Chem. Phys. Lett. 380 (2003) 245–250.
[28] W.J. Yang, L. Luo, T.M. Chen, N.S. Wang, Chem. Mater. 17 (2005) 3883–3888.
[29] W.B. Im, J.H. Kang, D.C. Lee, S. Lee, D.Y. Jeon, Y.C. Kang, K.Y. Jung, Solid State Commun. 133 (2005) 197–201.
[30] H. Ebendorff-Heidepriem, D. Ehrt, J. Phys. Condens. Matter 11 (1999) 7627–7634.
[31] K.B. Kim, Y.I. Kim, H.G. Chun, T.Y. Cho, J.S. Jung, J.G. Kang, Chem. Mater. 14 (2002) 5045–5052.
[32] K.Y. Jung, H.W. Lee, H.K. Jung, Chem. Mater. 18 (2006) 2249–2255.
[33] X.M. Liu, C.K. Lin, Y. Luo, J. Lin, J. Electrochem. Soc. 157 (2007) J21–J27.
[34] P.Y. Jia, X.M. Liu, G.Z. Li, M. Yu, J. Fang, J. Lin, Nanotechnology 17 (2006) 734–742.
[35] C. Feldman, Phys. Rev. 117 (1960) 455–457.
[36] D. Kumar, K.G. Cho, Z. Chen, V. Craciun, P.H. Holloway, R.K. Singh, Phys. Rev. B 60 (1999) 13331–13334.
[37] R.D. Shannon, Acta Crystallogr. Sect. A 32 (1976) 751–767.